Mineralogical Magazine (2019), **83**, 551–559
doi:10.1180/mgm.2018.157

CAMBRIDGE
UNIVERSITY PRESS

Article

Voudourisite, $Cd(SO_4)\cdot H_2O$, and lazaridisite, $Cd_3(SO_4)_3\cdot 8H_2O$, two new minerals from the Lavrion Mining District, Greece

Branko Rieck, Christian L. Lengauer and Gerald Giester*
Institut für Mineralogie und Kristallographie, Universität Wien – Geozentrum, Althanstraße 14, 1090 Wien, Austria

Abstract

Voudourisite, $Cd(SO_4)\cdot H_2O$, and lazaridisite, $Cd_3(SO_4)_3\cdot 8H_2O$, are two new minerals from the Esperanza Mine, Kaminiza Area, Lavrion Mining District, Greece. This small ancient mine is also the type locality of niedermayrite and katerinopoulosite. Further associated minerals are sphalerite, galena, edwardsite, chalcanthite, gypsum and greenockite. Both secondary minerals form tiny clusters or crusts and are among the latest to form in this paragenetic sequence. They are colourless or white, transparent to translucent, with a white streak and vitreous lustre. No fluorescence is observed. The minerals exhibit conchoidal fracture, no cleavage or preferred parting. The Mohs hardness is ~3 and both have brittle tenacity. Voudourisite is biaxial (–) with refractive indices at 589(1) nm of $\alpha = 1.580(2)$, $\beta = 1.624(2)$, $\gamma = 1.640(2)$, $2V_{meas.} = 70(5)°$, $2V_{calc.} = 61°$ and $\beta \sim \parallel$ [010]. Lazaridisite is biaxial neutral with refractive indices at 589(1) nm of $\alpha = 1.552(2)$, $\beta = 1.561(2)$, $\gamma = 1.570(2)$, $2V_{meas.} = 90(5)°$ and $2V_{calc.} = 90°$. The chemical compositions of voudourisite and lazaridisite are close to ideal with only minor amounts of copper detectable. The atomic arrangement in voudourisite (space group $P2_1/c$ with $a = 7.633(2)$, $b = 7.458(2)$, $c = 8.151(2)$ Å, $\beta = 122.35(1)°$ and $V = 392.0(2)$ Å^3) is related to that of kieserite while lazaridisite (space group $C2/c$ with $a = 14.813(3)$, $b = 11.902(2)$, $c = 9.466(2)$ Å, $\beta = 97.38(1)°$ and $V = 1655.2(6)$ Å^3) is a distinct structure-type. Calculated densities are 3.838 and 3.088 g/cm^3, respectively.

The strongest lines in the powder X-ray pattern [*d* in Å (I) (*hkl*)] are: 4.890 (66) (110); 3.741 (25) (020); 3.578 (100) (11$\bar{2}$); 3.230 (43) (200); 2.525 (33) (022); 2.395 (29) (112) for voudourisite and 6.860 (100) (200); 6.317 (72) (111); 5.965 (84) (020); 4.512 (58) (310); 3.727 (78) (202); 3.608(82)(13$\bar{1}$); 3.109 (83) (40$\bar{2}$); 3.020 (50) (33$\bar{1}$) for lazaridisite, respectively.

Keywords: voudourisite, lazaridisite, new mineral, cadmium sulfates, Lavrion Mining District, Greece

(Received 3 April 2018; accepted 2 September 2018; Accepted Manuscript online: 9 November 2018; Associate Editor: Michael Rumsey)

Introduction

The Lavrion Mining District, Greece, is part of the Attic–Cycladic–Pelagonian ore belt, and includes – apart from Lavrion – significant base- and precious-metal deposits in south Evia, Sifnos, Tinos and Kythnos (Vavelidis, 1997; Skarpelis, 2002; Tombros *et al.*, 2004; Neubauer, 2005; Tombros *et al.*, 2007). Several styles of sulfide mineralisation, including skarns, skarn-free carbonate replacement and vein-type ores, are found in the area (Voudouris, 2005). The Lavrion District is famous for its lead–zinc–silver ores that were mined in ancient times, most notably 600–400 B.C. and contributed to the wealth of Athens during the classical period. The district covers an area of ~150 km^2 at the southern tip of the Attica peninsula. Conophagos (1980) estimated that, until the depletion and closure of the mines, 2.3 million metric tons of lead and 7.800 tons of silver were extracted from the ores.

The area is also well-known for the occurrence of (up to now) ~580 mineral species, and it is the type locality of ~20 new minerals (Rieck *et al.*, 2018). The district has been the subject of intense investigation by the authors for more than two decades (Rieck, 1999; Rieck and Rieck, 1999; Rieck and Wendel, 1999; Wendel and Rieck, 1999*a*,*b*; Giester *et al.*, 2000; Giester *et al.*, 2007; Rieck, 2012; Giester and Rieck, 2014; Kolitsch *et al.*, 2014*a*,*b*; Kolitsch *et al.*, 2015). Several new mineral species have been described by our research group, i.e. mereiterite, $K_2Fe^{2+}(SO_4)_2\cdot 4H_2O$ (Giester and Rieck, 1995), niedermayrite, $Cu_4Cd(SO_4)_2(OH)_6\cdot 4H_2O$ (Giester *et al.*, 1998), kapellasite, $Cu_3Zn(OH)_6Cl_2$ (Krause *et al.*, 2006), and a secondary zinc mineral phase with the formula $Zn_9(SO_4)_2(OH)_{12}Cl_2\cdot 6H_2O$ (Kolitsch and Giester, 2013). In addition two minerals have been approved recently: prachařite, $CaSb_2^{5+}(As_2^{3+}O_3)_4\cdot 10H_2O$, (IMA2018-081, Kolitsch *et al.*, 2018) and $CaZn_2(AsO_4)_2\cdot 4H_2O$, (IMA2018-051a, Rieck *et al.*, 2019). The paragenesis of niedermayrite (at the Esperanza Mine, Kaminiza Area) was further studied in detail (Rieck, 2012) on freshly excavated rocks revealing colourless crusts of water-soluble minerals (Fig. 1), which previously had been eliminated on some old niedermayrite specimens due to ultrasonic cleaning in water. These colourless grains were studied by single-crystal and powder X-ray diffraction as well as electron microprobe analysis and are new minerals of chemically simple composition $Cd(SO_4)\cdot H_2O$ (voudourisite), and $Cd_3(SO_4)_3\cdot 8H_2O$ (lazaridisite). The crystal structures of the respective isotypic synthetic sulfates have been described already by Brégeault and Herpin (1970), Theppitak and Chainok (2015), Lipson (1936)

***Author for correspondence:** Gerald Giester, Email: gerald.giester@univie.ac.at
Cite this article: Rieck B., Lengauer C.L. and Giester G. (2019) Voudourisite, Cd(SO_4)·H_2O, and lazaridisite, $Cd_3(SO_4)_3\cdot 8H_2O$, two new minerals from the Lavrion Mining District, Greece. *Mineralogical Magazine* **83**, 551–559. https://doi.org/10.1180/mgm.2018.157

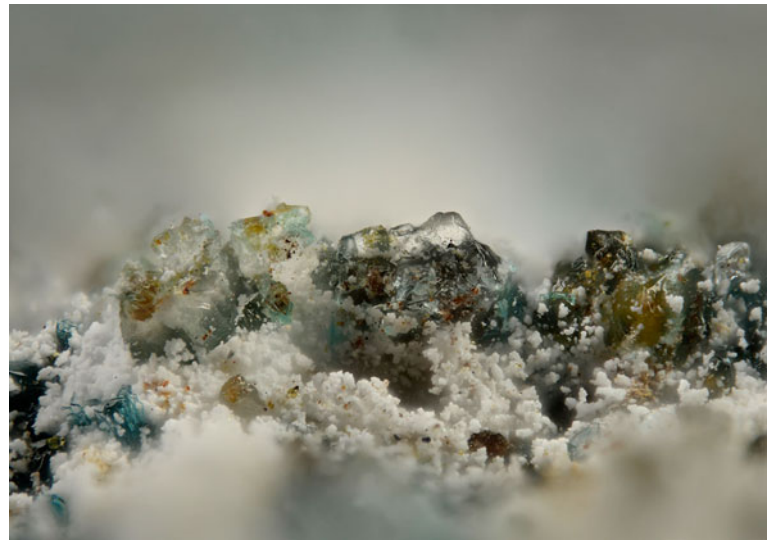

Fig. 1. Clear lazaridisite, white powdery voudourisite and blue–green niedermayrite from the #19 Mine, Ano Sounio, Lavrion, Field of view: 1.5 mm. Photo: H. Schillhammer. Private collection, B. Rieck, specimen no. S19108-0010.

and Caminiti and Johansson (1981). A cadmium sulfate monohydrate was described from Radvanice, Czech Republic, by Sejkora and Kotrlý (1998). The Radvanice occurrence, however, does not fulfil the criteria for acceptance as a new mineral as it was reported to be the efflorescence from a burning coal dump. Another new cadmium sulfate tetrahydrate, $Cd(SO_4)\cdot 4H_2O$ (drobecite), also mentioned from the Esperanza Mine (Giester and Rieck, 2010), is unfortunately poorly characterised. Voudourisite and lazaridisite have since been observed in Lavrion at the #19 Mine in the Ano Sounio area and at the North Mine in the Villia area, with the finds at #19 Mine enabling a full description of the two new species.

Mineral names and type material

Voudourisite is named in honour of Professor Panagiotis Voudouris (born 1962), Department of Mineralogy and Petrology, Faculty of Geology and Geoenvironment, National and Kapodistrian University of Athens, in recognition of his groundbreaking work on the Lavrion deposits. Lazaridisite is named after Stathis Lazaridis (1953–2010), a mineral collector from Lavrion, who contributed significantly to our current understanding of the paragenetic sequences within the Lavrion deposits.

Both minerals and their names have been approved by the Commission on New Minerals, Nomenclature and Classification of the International Mineralogical Association under numbers IMA2012-042 (Rieck and Giester, 2012*a*) and IMA2012-043 (Rieck and Giester, 2012*b*), respectively. The type specimen for both minerals is deposited in the collection of the Institut für Mineralogie und Kristallographie, University of Vienna, Althanstraße 14, 1090 Wien, Austria, catalogue number HS13.077.

Occurrence

Both newly described minerals originate from the type locality of niedermayrite (Fig. 2) at the Esperanza Mine, Kaminiza Area, Lavrion Mining District, Attica, Greece. This small ancient mine is situated ~2.5 km NW of the town of Lavrion, close (<1 km) to the well-known 'Km 3' site along the road to Agios Konstantinos. The recent finds have been made at the #19 Mine (Ano Sounio area) and the North Mine (Villia area). At both localities, the two new minerals are associated with sphalerite, galena, niedermayrite, edwardsite, chalcanthite, gypsum and greenockite. Voudourisite and lazaridisite are secondary minerals formed as the result of the weathering of the primary cadmium sulfides hawleyite and greenockite (cf. Rieck, 2012) and are among the latest to form in this paragenetic sequence.

Appearance, physical and optical properties

The two minerals form tiny clusters of stacked, short prismatic and rounded crystals on the sulfide minerals of the assemblage. Voudourisite also appears as powdery coatings covering areas of several square centimetres at the #19 Mine.

While neither cleavage nor preferred parting has been observed, the minerals exhibit conchoidal fracture. The Mohs hardness is ~3 and both have brittle tenacity. Densities were measured using micro-pycnometry (bromoform-filled capillary with an inner diameter of 0.5 mm and a length of 10 cm) to be 3.80(5) g/cm^3 (voudourisite) and 3.10(5) g/cm^3 (lazaridisite). These values compare well with the calculated densities of 3.838 and 3.089 g/cm^3, respectively, based on the empirical chemical formula and the unit-cell dimensions obtained from single-crystal X-ray diffraction.

Both minerals are colourless or white, show transparent to translucent diaphaneity and have a vitreous lustre; the streak is white. No fluorescence was observed in either longwave or shortwave ultraviolet illumination.

Mineral fragments were mounted on glass fibres and inspected under a Leitz Ortholux polarising microscope equipped with a Trelle micro-refractometer spindle stage using Cargille liquids (Series A: 1.460–1.640, Δn: 0.002). The optical angle and orientation of the optical axis were based on extinction data evaluated with the software *EXCALIBR* (Gunter *et al.*, 2004). Voudourisite is biaxial (–) with refractive indices at 589(1) nm of $\alpha = 1.580(2)$, $\beta = 1.624(2)$, $\gamma = 1.640(2)$, $2V_{meas.} = 70(5)°$, $2V_{calc.} = 61°$ and $\beta \sim ||$ [010]. Lazaridisite is biaxial neutral with refractive indices at 589(1) nm of $\alpha = 1.552(2)$, $\beta = 1.561(2)$, $\gamma = 1.570(2)$, $2V_{meas.} = 90(5)°$ and $2V_{calc.} = 90°$. Calculating K_c for the empirical formulae using the Gladstone-Dale relationship (Gladstone and Dale, 1863) with the values given by Mandarino (1976), combined with the optical data, resulted in a compatibility index for the empirical formula of 0.004 (voudourisite) and 0.008 (lazaridisite),

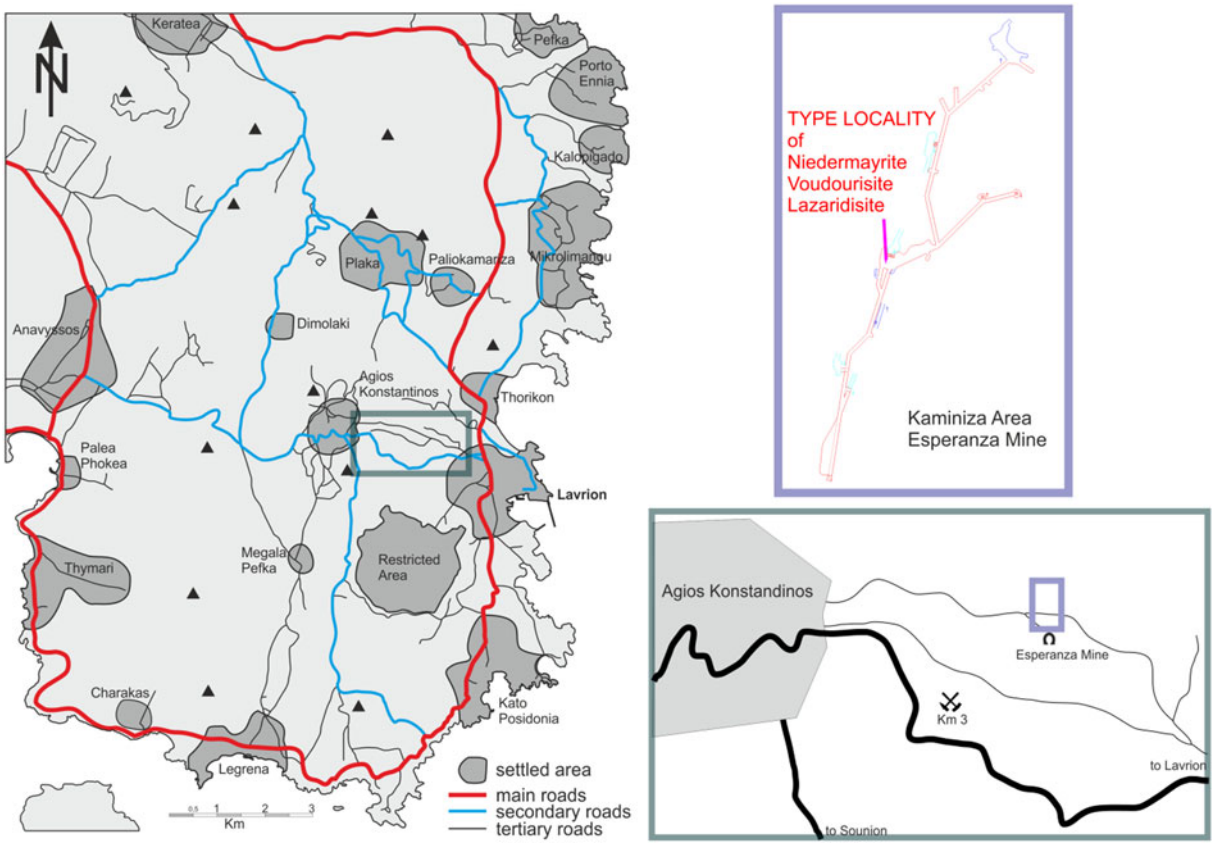

Fig. 2. Type locality of cadmium-bearing minerals within the Esperanza Mine. Mapping by K.H. Fabritz.

which is rated as superior (Mandarino, 1981). Both species show no discernible pleochroism.

Chemical composition

Chemical analyses (6 spots for voudourisite and 9 for lazaridisite) were done using an electron microprobe JEOL JXA-8500F (energy-dispersive spectroscopy mode, 20 kV, 20 nA, 5–6 µm beam diameter). The size and scarcity of the crystals did not allow direct measurement of H_2O; it was calculated by stoichiometry from the results of the crystal-structure analysis. No elements other than those reported were detected. Analytical data are given in Table 1.

The empirical formula for voudourisite (based on 5 O atoms per formula unit) is $(Cd_{0.81}Cu_{0.16}Fe_{0.04}Mg_{0.01})_{\Sigma 1.02}S_{0.99}O_4{\cdot}H_2O$. The simplified formula is $Cd(SO_4){\cdot}H_2O$, which requires CdO 56.69, SO_3 35.35, H_2O 7.96, total 100 wt.%.

The empirical formula for lazaridisite (based on 20 O atoms per formula unit) is $3(Cd_{0.86}Cu_{0.09}Fe_{0.04}Mg_{0.01})_{\Sigma 1.00}S_{1.00}O_4{\cdot}8H_2O$. The simplified formula is $Cd_3(SO_4)_3{\cdot}8H_2O$, which requires CdO 50.06, SO_3 31.21, H_2O 18.736, total 100 wt.%.

Powder X-ray diffraction

Measurements were carried out with a Philips PW3020 diffractometer using Cu*K*α radiation. At the time of the IMA proposals, only lazaridisite had precise data (Table 3). However, the recent finds of voudourisite from the #19 mine in Sounion have allowed a new measurement of powder diffraction data (Table 2) thus completing the preceding Gandolfi examinations. The *hkl* assignments of the Gandolfi measurement for voudourisite were done initially according to the known data for the synthetic material from ICDD entry 20-1411 (powder diffraction files from the International Centre for Diffraction Data, http://www.icdd.com/). The correct indexing of the new powder X-ray diffraction data (Holland and Redfern, 1997) in Tables 2 and 3 is based on the consistent unit-cell choices given in Table 4. The refined unit-cell parameters from these powder data are $a = 7.638(3)$, $b = 7.462(3)$, $c = 8.156(3)$ Å, $\beta = 122.41(3)°$ and $V = 392.4(2)$ Å^3 for voudourisite, and $a = 14.774(6)$, $b = 11.924(5)$, $c = 9.483(4)$ Å, $\beta = 97.70(3)°$ and $V = 1655.5(8)$ Å^3 for lazaridisite, both in good agreement to the values obtained from single-crystal X-ray work. The strongest lines in the powder X-ray pattern [*d* in Å (I) (*hkl*)] are: 4.890 (66) (110); 3.741 (25) (020); 3.578 (100) (11$\bar{2}$); 3.230 (43) (200); 2.525 (33) (022); 2.395 (29) (112) for voudourisite and 6.860, (100) (200); 6.317 (72) (111); 5.965 (84) (020); 4.512 (58) (310); 3.727 (78) (202); 3.608 (82) (13$\bar{1}$); 3.109 (83) (40$\bar{2}$); 3.020 (50) (33$\bar{1}$) for lazaridisite, respectively. The *d* values for both minerals compare very well with the data for the synthetic analogues (ICDD entries 20-1411, 53-841 and 20-187 for observed powder X-ray data).

Single-crystal X-ray diffraction data and crystal-structure refinements

Small fragments of voudourisite and lazaridisite were separated carefully for collection of single crystal X-ray diffraction data (Mo*K*α radiation, microcapillary optics) at room temperature on a Nonius KappaCCD diffractometer. Several sets of phi- and omega-scans

Table 1. Chemical compositions (wt.%) for voudourisite and lazaridisite.

	Voudourisite			Lazaridisite			Standard
Const.	Mean	Range	SD	Mean	Range	SD	
CdO	47.91	43.26–51.02	3.31	44.45	44.10–46.72	0.81	CdS
SO_3	36.43	35.02–36.77	0.63	31.98	32.01–31.66	0.11	$CaSO_4$
CuO	5.98	0.44–6.99	2.44	3.02	1.27–3.43	0.64	CuO
FeO	1.27	0.87–1.88	0.37	1.19	1.10–1.28	0.05	Fe_2O_3
MgO	0.22	0.19–0.33	0.05	0.16	0.0–0.27	0.08	MgO
H_2O*	8.28			19.26			
Total	100.09			100.06			

*Calculated on the basis of the crystal structure refinement and 5 (voudourisite) and 20 (lazaridisite) O atoms per formula unit.
Const. – constituent; SD – standard deviation.

Table 2. Powder X-ray diffraction data for voudourisite*.

I/I_{100}	I_{calc}	d_{obs}	d_{calc}	*h k l*
2	3	6.446	6.44826	1 0 0
2	1	5.075	5.06631	1 1 $\bar{1}$
9	5	5.057	5.06052	0 1 1
66	**64**	**4.890**	**4.87901**	1 1 0
3	2	4.078	4.07793	1 0 $\bar{2}$
25	**26**	**3.741**	**3.73110**	0 2 0
100	**100**	**3.578**	**3.57845**	1 1 $\bar{2}$
2	3	3.457	3.45021	2 0 $\bar{2}$
7	5	3.443	3.44291	0 0 2
6	5	3.379	3.39089	2 1 $\bar{1}$
15	15	3.292	3.28204	1 2 $\bar{1}$
43	**45**	**3.230**	**3.22413**	2 0 0
13	13	3.130	3.13167	2 1 $\bar{2}$
5	4	2.965	2.95969	2 1 0
2	3	2.755	2.75275	1 2 $\bar{2}$
5	4	2.655	2.66205	1 2 1
11	10	2.531	2.53315	2 2 $\bar{2}$
33	**32**	**2.525**	**2.53026**	0 2 2
3	1	2.506	2.50465	1 1 $\bar{3}$
10	8	2.439	2.43951	2 2 0
9	7	2.396	2.39776	3 1 $\bar{2}$
29	**30**	**2.395**	**2.39286**	1 1 2
15	17	2.318	2.32072	1 3 0
2	2	2.150	2.14942	3 0 0
14	13	2.122	2.12353	1 3 $\bar{2}$
6	7	2.098	2.09514	3 2 $\bar{2}$
1	4	2.069	2.06544	3 1 0
12	11	2.051	2.05431	3 2 $\bar{1}$
7	5	2.040	2.03896	2 0 $\bar{4}$
2	3	2.018	2.01771	2 3 $\bar{2}$
2	1	1.971	1.96942	2 3 0
3	2	1.969	1.96686	2 1 $\bar{4}$
2	3	1.943	1.94540	3 0 $\bar{4}$
2	5	1.898	1.89962	2 0 2
4	5	1.886	1.88248	3 1 $\bar{4}$
5	3	1.877	1.88011	1 1 $\bar{4}$
2	4	1.863	1.86555	0 4 0
4	7	1.847	1.84425	4 1 $\bar{2}$
3	6	1.789	1.78923	2 2 $\bar{4}$
7	7	1.774	1.77244	1 3 2
7	5	1.724	1.72500	3 2 $\bar{4}$
3	7	1.721	1.72145	0 0 4
7	6	1.696	1.69544	4 2 $\bar{2}$
5	5	1.692	1.69284	2 2 2
4	1	1.687	1.68684	0 3 3
1	2	1.678	1.68077	4 1 $\bar{4}$
5	7	1.642	1.64102	2 4 $\bar{2}$
9	9	1.642	1.64023	0 4 2
7	7	1.624	1.62634	3 3 0
2	1	1.610	1.61206	4 0 0
4	2	1.577	1.57572	4 1 0
4	6	1.565	1.56311	0 2 4

*Intensities were calculated using *VESTA 3* (Momma and Izumi, 2011); the strongest lines are given in bold.

Table 3. Powder X-ray diffraction data for lazaridisite*.

I/I_{100}	I_{calc}	d_{obs}	d_{calc}	*h k l*
10	15	7.335	7.32039	2 0 0
100	**100**	**6.860**	**6.88861**	1 1 $\bar{1}$
72	**70**	**6.317**	**6.32846**	1 1 1
84	**75**	**5.965**	**5.96177**	0 2 0
17	12	5.023	5.03426	0 2 1
15	7	4.682	4.69897	0 0 2
9	13	4.617	4.62270	2 2 0
58	**56**	**4.512**	**4.51658**	3 1 0
38	33	4.335	4.33993	1 1 $\bar{2}$
28	31	4.302	4.28355	3 1 $\bar{1}$
3	5	4.216	4.21979	2 0 $\bar{2}$
2	6	4.065	4.05274	1 1 2
24	29	4.027	4.01564	2 2 1
78	**73**	**3.727**	**3.73349**	2 0 2
17	7	3.660	3.66020	4 0 0
82	75	3.608	3.59573	1 3 $\bar{1}$
40	34	3.498	3.50846	1 3 1
10	5	3.472	3.47896	3 1 $\bar{2}$
10	16	3.437	3.44431	2 2 $\bar{2}$
43	36	3.164	3.16423	2 2 2
83	**76**	**3.109**	**3.09566**	4 0 $\bar{2}$
12	19	3.058	3.06700	4 2 $\bar{1}$
2	2	3.037	3.02388	1 3 $\bar{2}$
50	**51**	**3.020**	**3.00462**	3 3 $\bar{1}$
16	10	2.968	2.98089	0 4 0
33	42	2.903	2.89347	1 1 3
3	3	2.838	2.84366	5 1 0
5	10	2.828	2.82563	5 1 $\bar{1}$
14	19	2.768	2.76077	2 4 0
11	17	2.750	2.74736	4 2 $\bar{2}$
13	7	2.733	2.73802	3 1 $\bar{3}$
17	18	2.725	2.71648	4 0 2
6	2	2.682	2.68324	3 3 $\bar{2}$
13	10	2.621	2.62862	5 1 1
23	20	2.617	2.61337	2 4 1
11	3	2.496	2.49701	2 2 3
2	6	2.472	2.47196	4 2 2
3	4	2.438	2.44013	6 0 0
8	7	2.437	2.43469	2 4 $\bar{2}$
28	26	2.394	2.38560	1 3 3
5	3	2.358	2.35369	1 5 0
4	6	2.347	2.34715	5 3 $\bar{1}$
7	9	2.330	2.32948	2 4 2
15	5	2.310	2.31135	4 4 0
6	9	2.302	2.30368	5 1 2
6	14	2.257	2.25829	6 2 0
20	22	2.232	2.23052	5 3 1
13	4	2.191	2.19898	3 1 $\bar{4}$
14	9	2.164	2.16997	2 2 $\bar{4}$
9	11	2.146	2.14259	3 5 0
7	10	2.129	2.12518	2 4 $\bar{3}$
4	5	2.114	2.10990	4 0 $\bar{4}$
13	22	2.097	2.09402	4 2 3
10	23	1.988	1.98961	5 3 $\bar{3}$
22	3	1.980	1.98114	5 1 3
13	10	1.890	1.88941	6 4 $\bar{1}$
5	3	1.863	1.86257	1 5 3
8	9	1.846	1.86257	1 5 3
8	1	1.819	1.81710	3 1 $\bar{5}$
8	5	1.813	1.81221	1 1 5
7	10	1.795	1.79261	0 2 5
14	5	1.749	1.74623	2 4 4
14	10	1.693	1.69236	6 4 2
6	12	1.680	1.68165	8 2 1
16	11	1.667	1.66868	3 3 $\bar{5}$
2	6	1.661	1.66070	1 7 1
12		1.620	1.61825	8 2 $\bar{3}$

*Intensities were calculated using *VESTA 3* (Momma and Izumi, 2011); the strongest lines are given in bold.

Table 4. Crystal data and details of the single-crystal intensity measurement and structure refinement for voudourisite and lazaridisite.

	Voudourisite	Lazaridisite
Crystal data		
Formula	$Cd(SO_4)\cdot H_2O$	$Cd_3(SO_4)_3\cdot 8H_2O$
Crystal system, space group	Monoclinic, $P2_1/c$	Monoclinic, $C2/c$
Temperature (K)	296	296
a (Å)	7.633(2)	14.813(3)
b (Å)	7.458(2)	11.902(2)
c (Å)	8.151(2)	9.466(2)
β (°)	122.35(1)	97.38(1)
V (Å^3)	392.0(2)	1655.2(6)
Z	4	4
Calculated density (g/cm^3)	3.838	3.088
μ (Mo$K\alpha$) (mm^{-1})	6.00	4.30
Data collection		
Instrument	Nonius KappaCCD diffractometer	Nonius KappaCCD diffractometer
Radiation type, wavelength (Å)	Mo$K\alpha$, λ = 0.71073	Mo$K\alpha$, λ = 0.71073
Number of frames	403	377
Absorption correction	Multi-scan	Multi-scan
No. of measured, independent and observed [I >2σ(I)] reflections	2252, 1193, 1034	4905, 2512, 2145
R_{int}	0.014	0.018
Indices range of h, k, l	$-10 \le h \le 10$, $-10 \le k \le 10$, $-11 \le l \le 11$	$-21 \le h \le 21$, $-16 \le k \le 16$, $-13 \le l \le 13$
Refinement		
Refinement	Full-matrix least-squares	Full-matrix least-squares
Number of reflections, parameters, restraints	1193, 73, 2	2512, 144, 12
R_1 [for F_o>4σ(F_o)]*	0.0184	0.0199
wR_2 [for all F_o^2]*	0.0405	0.0440
$2\theta_{max}$ (°)	61	61
GoF	1.11	1.09
a, b**	0.0142, 0.25	0.019, 0.85
$\Delta\rho_{min\ /\ max}$ (e^- Å^{-3})	−0.62 / 0.93	−0.69 / 0.99

*$R_1 = \Sigma F_o - F_c / \Sigma F_o$; $wR_2 = [\Sigma w(F_o^2 - F_c^2)^2 / \Sigma w(F_o^2)^2]^{1/2}$;
**$w = 1 / [\sigma^2(F_o^2) + (a \times P)^2 + b \times P]$; $P = \{[\text{max of } (0 \text{ or } F_o^2)] + 2F_c^2\} / 3$

Table 5. Compilation of unit-cell choices from literature used for kieserite, compared with voudourisite and related compounds.

Formula	Kieserite $Mg(SO_4)\cdot H_2O$		Voudourisite $Cd(SO_4)\cdot H_2O$				Poitevinite $(Cu,Fe)(SO_4)\cdot H_2O$	
Space group	$C2/c$		$P2_1/n$		$P2_1/c$		$P\bar{1}$	"$C2/c$"
a (Å)	6.891	6.891	7.623	7.633	7.623	7.633	5.120	7.094
b (Å)	7.624	7.624	7.458	7.458	7.458	7.458	5.160	7.440
c (Å)	7.549	7.645	7.633	7.623	8.151	8.151	7.535	7.824
α (°)	90	90	90	90	90	90	107.06	89.47
β (°)	116.26	117.70	115.41	115.41	122.24	122.35	107.40	119.56
γ (°)	90	90	90	90	90	90	92.73	90.45
V (Å^3)	355.6	355.6	392.0	392.0	392.0	392.0	179.59	359.18
Z	4	4	4	4	4	4	2	4
Choice	R	K	A	B	K	C	D	K
a	(100)	(100)	(100)	(001)	(100)	(001)	(100)	(110)
b	(010)	(0$\bar{1}$0)	(010)	(0$\bar{1}$0)	(0$\bar{1}$0)	(0$\bar{1}$0)	(010)	(1$\bar{1}$0)
c	(001)	($\bar{1}$0$\bar{1}$)	(001)	(100)	($\bar{1}$0$\bar{1}$)	($\bar{1}$0$\bar{1}$)	(001)	($\bar{1}\bar{1}\bar{1}$)

R: 'Reduced' monoclinic setting. Kieserite-type sulfates (Le Fur *et al.*, 1966)
K: Kieserite (Leonhardt and Weiss, 1957; Brégault *et al.*, 1970; Hawthorne *et al.*, 1987), kieserite-type sulfates and selenates (Wildner and Giester, 1991; Giester and Wildner, 1992; Bechtold and Wildner, 2016) or atomic arrangement according to kieserite.
A: based on reduced unit cell with monoclinic setting
B: voudourisite (original submission: IMA2012-042)
C: voudourisite (present study); $Cd(SO_4)\cdot H_2O$ (Brégault and Herpin, 1970; Theppitak and Chainok, 2015); $Hg(SeO_4)\cdot H_2O$ and $Cd(SeO_4)\cdot H_2O$ (Stålhandske, 1978; 1981)
D: poitevinite (reduced unit cell, Giester *et al.*, 1994)

with 2° scan width (total 403/377 frames, 100/220 s/frame for voudourisite and lazaridisite, respectively) were measured at a crystal-to-detector distance of 30 mm up to 61°2θ. The absorption was corrected by evaluation of partial multi-scans. Selected crystal parameters and a summary of data collection and structure refinements for both minerals are given in Table 4. The atomic coordinates reported for synthetic $Cd_3(SO_4)_3\cdot 8H_2O$ (Caminiti and Johansson, 1981) were used as starting parameters for lazaridisite. For the

Table 6. Atom coordinates and displacement parameters with estimated standard deviations in parentheses for voudourisite and lazaridisite.*

	x	y	z	$U_{iso/eq}$	U^{11}	U^{22}	U^{33}	U^{23}	U^{13}	U^{12}
Voudourisite										
Cd	0.21883(3)	0.26010(2)	0.26059(2)	0.01395(8)	0.01228(11)	0.01446(11)	0.01256(12)	0.00078(6)	0.00496(9)	−0.00163(6)
S	0.25516(8)	0.61731(7)	0.01222(8)	0.01118(12)	0.0094(2)	0.0093(2)	0.0120(3)	0.0007(2)	0.0038(2)	0.0001(2)
O1	0.1375(3)	0.5001(2)	−0.1580(2)	0.0188(4)	0.0176(9)	0.0170(8)	0.0157(9)	−0.0046(7)	0.0048(8)	−0.0005(7)
O2	0.1104(3)	0.7597(2)	−0.0049(3)	0.0168(4)	0.0124(9)	0.0127(8)	0.0209(10)	−0.0020(6)	0.0059(8)	0.0029(6)
O3	0.3279(2)	0.5129(2)	0.1922(2)	0.0173(4)	0.0154(9)	0.0165(8)	0.0140(9)	0.0046(7)	0.0039(7)	−0.0022(7)
O4	0.4339(3)	0.6998(2)	0.0214(3)	0.0186(4)	0.0111(8)	0.0224(8)	0.0185(9)	0.0033(7)	0.0056(7)	−0.0032(7)
O5	0.2758(3)	0.0976(2)	0.0385(2)	0.0146(3)	0.0118(8)	0.0148(8)	0.0147(8)	−0.0001(7)	0.0054(7)	0.0000(7)
H1	0.400(3)	0.075(4)	0.104(4)	0.035(9)						
H2	0.220(4)	−0.008(3)	0.005(4)	0.034(9)						
Lazaridisite										
Cd1	0.15448(2)	0.40515(2)	0.03508(2)	0.01690(6)	0.01487(9)	0.01995(10)	0.01608(9)	−0.00062(6)	0.00275(6)	−0.00056(6)
Cd2	0	−0.05374(2)	¼	0.01658(7)	0.01509(11)	0.01803(12)	0.01626(11)	0	0.00066(8)	0
S1	0	0.50823(6)	¼	0.01220(14)	0.0117(3)	0.0140(3)	0.0108(3)	0	0.0006(2)	0
S2	0.12975(3)	0.11689(4)	0.05632(5)	0.01275(11)	0.0117(2)	0.0154(2)	0.0112(2)	0.00018(18)	0.00182(18)	−0.00030(19)
O1	0.02578(11)	0.43560(13)	0.13553(16)	0.0200(3)	0.0203(8)	0.0227(8)	0.0179(7)	−0.0060(6)	0.0057(6)	−0.0006(6)
O2	0.42242(11)	0.07973(13)	0.19345(16)	0.0205(3)	0.0177(8)	0.0247(8)	0.0180(8)	0.0026(6)	−0.0022(6)	0.0071(6)
O3	0.39627(11)	0.47077(13)	0.05167(16)	0.0205(3)	0.0229(8)	0.0192(8)	0.0179(8)	−0.0045(6)	−0.0028(6)	0.0017(7)
O4	0.10086(12)	0.22669(13)	−0.00324(17)	0.0227(4)	0.0250(9)	0.0160(8)	0.0249(9)	0.0041(6)	−0.0055(7)	−0.0007(6)
O5	0.08508(11)	0.09405(13)	0.18368(16)	0.0212(3)	0.0229(8)	0.0249(9)	0.0174(8)	−0.0009(6)	0.0092(6)	−0.0059(7)
O6	0.22897(10)	0.11514(14)	0.09781(17)	0.0212(3)	0.0123(8)	0.0323(9)	0.0184(8)	−0.0026(7)	0.0005(6)	0.0011(6)
O7	0.09340(11)	0.19322(14)	0.68234(17)	0.0224(3)	0.0235(9)	0.0234(8)	0.0201(8)	0.0019(7)	0.0024(7)	−0.0006(7)
O8	0.27877(12)	0.07487(14)	0.40187(18)	0.0255(4)	0.0286(10)	0.0258(9)	0.0222(9)	0.0029(7)	0.0038(7)	0.0022(7)
O9	0.22167(12)	0.35826(16)	0.25726(18)	0.0292(4)	0.0227(9)	0.0384(11)	0.0255(9)	0.0090(8)	−0.0008(7)	0.0013(8)
O10	0.09536(12)	0.25078(14)	0.40727(18)	0.0244(3)	0.0260(9)	0.0236(9)	0.0233(8)	−0.0007(7)	0.0016(7)	0.0017(7)
H1	0.082(2)	0.2568(14)	0.726(2)	0.034						
H2	0.092(2)	0.214(2)	0.5921(12)	0.034						
H3	0.2211(9)	0.065(2)	0.411(3)	0.038						
H4	0.2836(19)	0.075(3)	0.3102(13)	0.038						
H5	0.1887(15)	0.316(2)	0.308(3)	0.044						
H6	0.2789(8)	0.337(2)	0.284(3)	0.044						
H7	0.0771(18)	0.1968(17)	0.346(3)	0.037						
H8	0.0518(14)	0.3012(17)	0.399(3)	0.037						

*Site symmetries (with Wyckoff positions in parentheses) are 1 (4*e*) resp. (8*f*) for all atoms except 2 (4*e*) for Cd2 and S1. For lazaridisite, the geometry of hydrogen atoms was refined with soft restrictions and U_{iso} values fixed to 1.5 times U_{eq} of the parent oxygen atom.

description of voudourisite, the unit-cell setting in space group $P2_1/c$ was chosen (*cf.* Table 5) and initial values for the atomic parameters according to Brégault and Herpin (1970) and Theppitak and Chainok (2015). The crystal structures were refined by full-matrix least-squares techniques using *SHELXL97* (Sheldrick, 2008). A substitution of Cd by Cu could not be proven reliably by the structure refinements (Cu < 2%), and was therefore ignored. Final atom positions and important interatomic distances and angles are listed in Tables 6 and 7, respectively. Details on the hydrogen-bond schemes are summarised in Table 8.

Table 7. Selected interatomic distances (Å) and angles (°) for voudourisite and lazaridisite.

Voudourisite					
Cd–O1	2.2436(17)	S–O1	1.4703(18)	O4–S–O1	112.38(11)
Cd–O2	2.253(2)	S–O2	1.4842(17)	O4–S–O3	109.02(10)
Cd–O3	2.2481(16)	S–O3	1.4819(18)	O1–S–O3	109.76(11)
Cd–O4	2.312(2)	S–O4	1.4620(18)	O4–S–O2	109.35(10)
Cd–O5	2.3223(18)	<S–O>	<1.475>	O1–S–O2	106.75(10)
Cd–O5	2.4036(17)			O3–S–O2	109.54(11)
<Cd–O>	<2.297>			<O–S–O>	<109.47>
Lazaridisite					
Cd1–O1	2.2662(16)	S2–O3	1.4767(16)	O4–S2–O5	109.86(10)
Cd1–O2	2.3189(16)	S2–O4	1.4653(16)	O4–S2–O6	110.34(10)
Cd1–O4	2.2803(16)	S2–O5	1.4731(16)	O5–S2–O6	108.48(9)
Cd1–O6	2.2758(16)	S2–O6	1.4720(16)	O4–S2–O3	109.05(9)
Cd1–O8	2.2942(18)	<S2–O>	<1.472>	O5–S2–O3	109.36(9)
Cd1–O9	2.2777(17)			O6–S2–O3	109.73(9)
<Cd1–O>	<2.286>			<O–S2–O>	<109.47>
Cd2–O3 ×2	2.2869(16)	S1–O1 ×2	1.4743(15)	O2–S1–O2	109.49(14)
Cd2–O5 ×2	2.2978(15)	S1–O2 ×2	1.4743(16)	O2–S1–O1 ×2	109.99(9)
Cd2–O7 ×2	2.3039(17)	<S1–O>	<1.4743>	O2–S1–O1 ×2	109.57(9)
<Cd2–O>	<2.296>			O1–S1–O1	108.20(13)
				<O–S1–O>	<109.47>

Structure descriptions

Voudourisite, $Cd(SO_4)\cdot H_2O$, belongs to the kieserite group $M(SO_4)\cdot H_2O$, with M = Mg (kieserite), Mn (szmikite), Fe (szomolnokite), Co (cobaltkieserite), Ni (dwornikite), Zn (gunningite) and Cu/Fe (poitevinite), listed as subdivision 7.CB of the Strunz Mineralogical Tables (Strunz and Nickel, 2001). Except for poitevinite and voudourisite, these minerals crystallise in the monoclinic space group $C2/c$ (Leonhardt and Weiss, 1957; Brégeault and Herpin, 1970; Hawthorne *et al.*, 1987; Wildner and Giester, 1991; Holtstam, 2002), as do the synthetic compounds $M(SeO_4)\cdot H_2O$ where M = Mg, Mn, Co, Ni or Zn (Giester and Wildner, 1992). Poitevinite (Giester *et al.*, 1994) is triclinic $P\overline{1}$, as observed for $Cu(XO_4)\cdot H_2O$ with X = S or Se (Giester, 1988). Voudourisite crystallises in the space group $P2_1/c$, a subgroup of $C2/c$, and is isotypic with $Hg(SeO_4)\cdot H_2O$ and $Cd(SeO_4)\cdot H_2O$ (Stålhandske, 1978; 1981). Several solid-solution series occur between end-members of the kieserite group, some of them (i.e. those incorporating copper) accompanied by a reduction of crystal symmetry (Cu/Fe: Giester *et al.*, 1994; Cu/Mg: Lengauer and Giester, 1995; Mg/Co: Bechtold and Wildner, 2016; or Mg/Fe: Talla and Wildner, 2017). The kieserite structure type

Table 8. Hydrogen-bonding schemes (Å, °) in voudourisite and lazaridisite.

D	H	*D*–H	*A*	*D*···*A*	*D*–H···*A*	*H*–D–*H*
Voudourisite						
O5	H1	0.82(2)	O3	2.695(3)	165(3)	102(3)
O5	H2	0.87(2)	O2	2.755(2)	166(3)	
Lazaridisite						
O7	H1	0.89(1)	O2	2.968(2)	167(2)	103(2)
O7	H2	0.89(1)	O10	2.696(2)	174(3)	
O8	H3	0.88(1)	O3	2.957(2)	155(3)	108(2)
O8	H4	0.88(1)	O6	2.918(2)	150(3)	
O9	H5	0.88(1)	O10	2.799(3)	167(3)	105(2)
O9	H6	0.89(1)	O7	2.794(2)	171(3)	
O10	H7	0.88(1)	O5	2.811(2)	156(3)	106(2)
O10	H8	0.88(1)	O1	2.835(2)	167(3)	

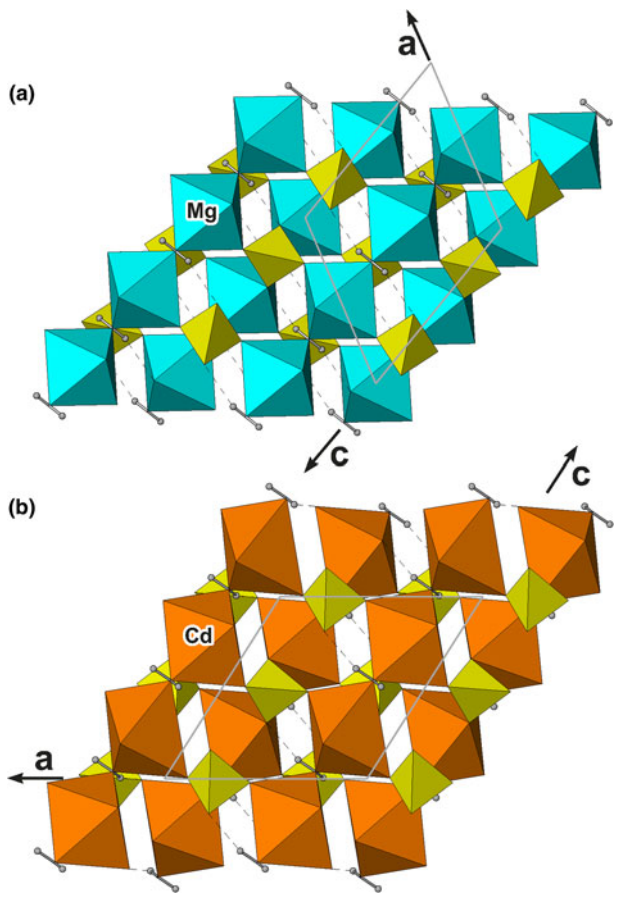

Fig. 3. Atomic arrangement in (*a*) kieserite and (*b*) voudourisite in projections on (010). All crystal structure drawings are done with *ATOMS* (Dowty, 2016).

is also known for some phosphates and arsenates with trivalent cations (e.g. Fe^{3+}, Mn^{3+} or V^{3+}), including serrabrancaite, $Mn(PO_4)\cdot H_2O$ (Witzke *et al.*, 2000); close structure relations are further evident with amblygonite, lazulite and titanite.

The atomic arrangement in kieserite-group minerals is characterised by a framework structure, composed by a corner-linkage of $MO_4(H_2O)_2$ octahedra and XO_4 tetrahedra, further strengthened by hydrogen bonding. The characteristic structure motif are chains of corner-sharing MO_6 octahedra (with H_2O molecules acting as bridging ligands) parallel to the [001] direction for unit-cell choice **K** according to kieserite (Fig 3*a*), for details see

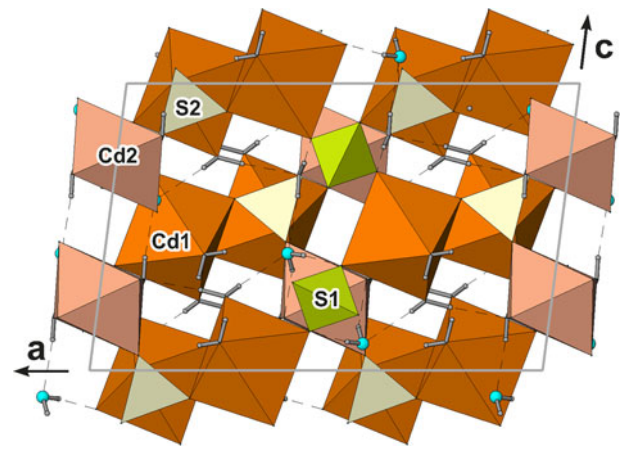

Fig. 4. Crystal structure of lazaridisite in a projection on (010).

the compilation in Table 5. In the present paper, we decided to describe voudourisite according to earlier literature on synthetic $Cd(SO_4)\cdot H_2O$ (Brégeault and Herpin, 1970; Theppitak and Chainok, 2015), and on isotypic $Hg(SeO_4)\cdot H_2O$ and $Cd(SeO_4)\cdot H_2O$ (Stålhandske, 1978; 1981), i.e. with respective chains arranged also along [001] but with **a** along [101] of kieserite (Fig. 3*b*). Differences in interatomic distances between synthetic $Cd(SO_4)\cdot H_2O$ (Theppitak and Chainok, 2015) and voudourisite are negligible with individual <Cd–O> and <S–O> distances ≤0.006 Å. In kieserite-type compounds with space group *C*2/*c* the atoms *M* (4*b*) and S, O3 (both 4*e*) are located on special positions with site symmetries of $\bar{1}$ and 2, respectively; in voudourisite ($P2_1/c$), all atoms have site symmetry 1, allowing a symmetry un-constrained variability of bond-length and bond-angle distortions. The Cd–O5 distances, i.e. those to the H_2O molecule, are the longest observed for the corresponding *M*–O3 distances (cf. Wildner and Giester, 1991).

The crystal structure of lazaridisite (*C*2/*c*) is a three-dimensional, heteropolyhedral framework of $CdO_4(H_2O)_2$ and SO_4 groups sharing common corners (Fig. 4) and one free H_2O molecule. Except Cd2 and S1 (both on 4*e* with site symmetry 2), all atoms are located on general sites. Again, differences of interatomic distances from the synthetic analogue $Cd_3(SO_4)_3\cdot 8H_2O$ (Caminiti and Johansson, 1981) are small, with individual <Cd–O> and <S–O> distances ≤0.01 Å. Both $CdO_4(H_2O)_2$ octahedra are moderately distorted, and contrary to voudourisite, the Cd–$O_{(H_2O)}$ bond lengths are similar to Cd–$O_{(SO_4)}$. For a detailed description of this structure type see Caminiti and Johansson (1981).

The hydrogen bonding schemes (Table 8) in voudourisite and lazaridisite are characterised by O–H···O distances ranging from 2.695–2.755 Å and 2.698–2.967 Å, respectively. Note that the hydrogen bond O5–H2···O2 in voudourisite is different to the local arrangement observed in kieserite.

Acknowledgements. The authors are grateful to Peter Leverett and two anonymous reviewers for helpful comments.

Supplementary material. To view supplementary material for this article, please visit https://doi.org/10.1180/mgm.2018.157

References

Bechtold A. and Wildner M. (2016) Crystal chemistry of the kieserite–cobalt-kieserite solid solution, $Mg_{1-x}Co_x(SO_4)\cdot H_2O$: well-behaved oddities. *European Journal of Mineralogy*, **28**, 43–52.

Brégeault J.M. and Herpin P. (1970) Etude structurale du sulfate de cadmium monohydrate $CdSO_4$ (H_2O). *Bulletin de la Societe Francaise de Mineralogie et de Cristallographie*, **93**, 37–42.

Caminiti R. and Johansson G. (1981) A refinement of the crystal structure of the cadmium sulfate $(CdSO_4)_3(H_2O)_8$. *Acta Chemica Scandinavica*, **35A**, 451–455.

Conophagos C.E. (1980) *Le Laurium Antique et la Technique Grecque de la Production de l'Argent*. Ekdotike Hellados S.A., Athens, Greece, 458 pp.

Dowty E. (2016) *Atoms V6.5.0 for Atomic Structure Display*. Shape Software, Kingsport, Tennessee, USA.

Giester G. (1988) The crystal structures of $CuSO_4{\cdot}H_2O$ and $CuSeO_4{\cdot}H_2O$, and their relationship to kieserite. *Mineralogy and Petrology*, **38**, 277–284.

Giester G. and Rieck B. (1995) Mereiterite, $K_2Fe[SO_4]_2{\cdot}4H_2O$, a new leonite-type mineral from the Lavrion Mining District, Greece. *European Journal of Mineralogy*, **7**, 559–566.

Giester G. and Rieck B. (2010) Drobecite, a novel mineral from the Lavrion, Greece, deposit. *Acta Mineralogica-Petrographica*, IMA 2010, Abstract Series 6, 20th General Meeting of the International Mineralogical Association, 21–27 August, Budapest, Hungary, 496.

Giester G. and Rieck B. (2014) Crystal structure refinement of aurichalcite, $(Cu,Zn)_5(CO_3)_2(OH)_6$, from the Lavrion Mining District, Greece. *Neues Jahrbuch für Mineralogie – Abhandlungen: Journal of Mineralogy and Geochemistry*, **191**, 225–232.

Giester G and Wildner M. (1992) The crystal structures of kieserite-type compounds. II. Crystal structures of $Me(II)SeO_4{\cdot}H_2O$ [Me = Mg, Mn, Co, Ni, Zn]. *Neues Jahrbuch für Mineralogie Monatshefte*, **1992**, 135–144.

Giester G., Lengauer C.L. and Redhammer G. (1994) Characterization of the $FeSO_4{\cdot}H_2O$ – $CuSO_4{\cdot}H_2O$ solid-solution series, and the nature of poitevinite, $(Cu,Fe)SO_4{\cdot}H_2O$. *The Canadian Mineralogist*, **32**, 873–884.

Giester G., Rieck B. and Brandstätter F. (1998) Niedermayrite, $Cu_4Cd(SO_4)_2(OH)_6{\cdot}4H_2O$, a new mineral from the Lavrion Mining District, Greece. *Mineralogy and Petrology*, **63**, 19–34.

Giester G., Lengauer C.L. and Rieck B. (2000) The crystal structure of nesquehonite, $MgCO_3{\cdot}3H_2O$, from Lavrion, Greece. *Mineralogy and Petrology*, **70**, 153–163.

Giester G., Kolitsch U., Leverett P., Turner P. and Williams P.A. (2007) The crystal structures of lavendulan, sampleite, and a new polymorph of sampleite. *European Journal of Mineralogy*, **19**, 75–93.

Gladstone J.H. and Dale T.P. (1863) Researches on the refraction, dispersion, and sensitiveness of liquids. *Philosophical Transactions of the Royal Society of London*, **153**, 317–343.

Gunter M.E., Bandli B.R., Bloss F.D., Evans S.H., Su S.-C. and Weaver R. (2004) Results from a McCrone spindle stage short course, a new version of EXCALIBR, and how to build a spindle stage. *The Microscope*, **52**, 23–39.

Hawthorne F.C., Groat L.A., Raudsepp M. and Ercit T.S. (1987) Kieserite, $Mg(SO_4){\cdot}(H_2O)$, a titanite-group mineral. *Neues Jahrbuch für Mineralogie Abhandlungen*, **157**, 121–132.

Holland T.J.B. and Redfern S.A.T. (1997) Unit cell refinement from powder diffraction data: the use of regression diagnostics. *Mineralogical Magazine*, **61**, 65–77.

Holtstam D. (2002) Cobaltkieserite, $CoSO_4{\cdot}H_2O$, a new mineral from Bastnäs, Skinnskatteberg, Sweden. *Geologiska Förenigens I Stockholm Förhandlinger*, **124**, 117–119.

Kolitsch U. and Giester G. (2013) The crystal structure of a new secondary zinc mineral from Lavrion, Greece: $Zn_9(SO_4)_2(OH)_{12}Cl_2{\cdot}6H_2O$. *Mitteilungen Österreichischen Mineralogischen Gesellschaft*, **159**, 74.

Kolitsch U., Rieck B., Brandstätter F., Schreiber F., Fabritz K.H., Blaß G. and Gröbner J. (2014*a*) Neufunde aus dem altem Bergbau und den Schlacken von Lavrion (I). *Mineralien-Welt*, **25**, 60–75.

Kolitsch U., Rieck B., Brandstätter F., Schreiber F., Fabritz K.H., Blaß G. and Gröbner J. (2014*b*): Neufunde aus dem altem Bergbau und den Schlacken von Lavrion (II). *Mineralien-Welt*, **25**, 82–95.

Kolitsch U., Rieck B. and Voudouris P. (2015) Mineralogy and genesis of the Lavrion ore deposit: new insights from the study of ore and accessory minerals. *Mitteilungen Österreichischen Mineralogischen Gesellschaft*, **161**, 66.

Kolitsch U., Sejkora J., Topa D., Kampf A.R., Plášil J., Rieck B. and Fabritz K.H. (2018) Prachařite, IMA 2018-081. CNMNC Newsletter No. 46, December 2018, page 1371; *Mineralogical Magazine*, **82**, 1369–1379.

Krause W., Bernhardt H.-J., Braithwaite R.S.W., Kolitsch U. and Pritchard R. (2006) Kapellasite, $Cu_3Zn(OH)_6Cl_2$, a new mineral from Lavrion, Greece. *Mineralogical Magazine*, **70**, 329–340.

Lengauer C.L. and Giester G. (1995) Rietveld refinement of the solid-solution series: $(Cu,Mg)SO_4{\cdot}H_2O$. *Powder Diffraction*, **10**, 189–194.

Le Fur Y., Coing-Boyat J. and Bassi G. (1966) Structure des sulfates monohydratés, monocliniques, des métaux de transition, MSO_4, H_2O (M = Mn, Fe, Co, Ni et Zn). *Comptes Rendus Academie Sciences Paris*, **262C**, 632–635.

Leonhardt J. and Weiss R. (1957) Das Kristallgitter des Kieserits $MgSO_4{\cdot}H_2O$. *Naturwissenschaften*, **44**, 338–339.

Lipson H. (1936) The crystal structure of $(CdSO_4)_3(H_2O)_8$. *Proceedings of the Royal Society of London, Series A: Mathematical and Physical Sciences*, **156**, 462–470.

Mandarino J.A. (1976) The Gladstone-Dale Relationship – Part I: Derivation of new constants. *The Canadian Mineralogist*, **14**, 498–502.

Mandarino J.A. (1981) The Gladstone-Dale Relationship: Part IV. The compatibility concept and its application. *The Canadian Mineralogist*, **19**, 441–450.

Momma K. and Izumi F. (2011) VESTA 3 for three-dimensional visualization of crystal, volumetric and morphology data. *Journal of Applied Crystallography*, **44**, 1272–1276.

Neubauer F. (2005) Structural control of mineralization in metamorphic core complexes. Pp. 561–564 in: *Mineral Deposit Research: Meeting the Global Challenge* (J. Mao and F.P. Bierlein, editors). Springer, Berlin.

Rieck B. (1999) Seltene Arsenate aus der Kamariza und weitere Neufunde. *LAPIS*, **24**, 68–76.

Rieck B. (2012) *Neue Minerale aus dem Lagerstätten-Bezirk Lavrion/Griechenland und den Kalahari Mangan Feldern/Republik Südafrika*. PhD dissertation, University of Vienna, Austria.

Rieck B. and Giester G. (2012*a*) Voudourisite, IMA 2012-042. CNMNC Newsletter No. 14, October 2012, page 1287; *Mineralogical Magazine*, **76**, 1281–1288.

Rieck B. and Giester G. (2012*b*) Lazaridisite, IMA 2012-043. CNMNC Newsletter No. 14, October 2012, page 1287; *Mineralogical Magazine*, **76**, 1281–1288.

Rieck B. and Rieck P. (1999) Silber, Arsen und Antimon: Vererzungen im Revier Plaka (Teil II). *LAPIS*, **24**, 59–63.

Rieck B. and Wendel W. (1999) Sounion – Hilarion Top aktuell: Funde vom Frühjahr '99. *LAPIS*, **24**, 77–78.

Rieck B., Kolitsch U., Voudouris P., Giester G. and Tzeferis P. (2018) Weitere Neufunde aus Lavrion. *Mineralien-Welt*, **29**, 32–77 [German].

Rieck B., Giester G., Lengauer C. and Topa D. (2019) IMA 2018-051a. CNMNC Newsletter No. 47, February 2019, page 146; *Mineralogical Magazine*, **83**, 143–147.

Sejkora J. and Kotrlý M. (1998) A new cadmium sulfate natural phase from Radvanice near Trutnov (Czech Republic). *Bulletin of the Czech Geological Survey*, **73**, 321–326.

Sheldrick G.M. (2008) A short history of SHELX. *Acta Crystallographica*, **64A**, 112–122.

Skarpelis N. (2002) Geodynamics and evolution of the Miocene mineralization in the Cycladic–Pelagonian belt, Hellenides. *Bulletin of the Geological Society of Greece*, **34**, 2191–2209.

Ståhlhandske C. (1978) A neutron diffraction study of mercury(II) selenate monohydrate. *Acta Crystallographica*, **34B**, 1408–1411.

Ståhlhandske C. (1981) Structure of cadmium selenate monohydrate. *Acta Crystallographica*, **37B**, 2055–2057.

Strunz H. and Nickel E.H. (2001) *Strunz Mineralogical Tables. Chemical-Structural Mineral Classification System*. 9th Edition, Schweitzerbart, Stuttgart, Germany

Talla D. and Wildner M. (2017) Crystal chemical and IR-spectroscopic investigation of the kieserite –szomolnokite solid solution series with relevance to Mars. *Mitteilungen Österreichischen Mineralogischen Gesellschaft*, **163**, 86.

Theppitak C. and Chainok K. (2015) Crystal structure of $CdSO_4(H_2O)$: a redetermination. *Acta Crystallographica*, **71E**, i8–i9.

Tombros S.F., Seymour K. and Spry P. (2004) Description and conditions of formation of new unnamed Ag-Cu and Ag-Cu-Au sulfotellurides in epithermal polymetallic Ag-Au-Te mineralization, Tinos Island, Hellas. *Neues Jahrbuch für Mineralogie Abhandlungen*, **179**, 295–310.

Tombros S.F., Seymour K., Williams-Jones A. and Spry P. (2007) The genesis of epithermal Au-Ag-Te mineralization, Panormos Bay, Tinos Island, Cyclades, Greece. *Economic Geology*, **102**, 1269–1294.

Vavelidis M. (1997) Au-bearing quartz veins and placer gold on Sifnos Island, Aegean Sea, Greece. Pp 335–338 in: *Mineral Deposits: Research and Exploration—Where do They Meet?* (H. Papunen, editor). Balkema, The Netherlands.

Voudouris P. (2005) Gold and silver mineralogy of the Lavrion deposit Attika/Greece. Pp 1089–1092 in: *Mineral Deposit Research: Meeting the Global Challenge* (J. Mao and F.P. Bierlein, editors) Springer, Berlin.

Wendel W. and Rieck B. (1999*a*) Die wichtigsten Mineralfundstellen Lavrions. *LAPIS*, **24**, 25–33.

Wendel W. and Rieck B. (1999*b*) Silber, Arsen und Antimon: Vererzungen im Revier Plaka (Teil I). *LAPIS*, **24**, 53–58.

Wildner M. and Giester G. (1991) The crystal structures of kieserite-type compounds. I. Crystal structures of $Me(II)SO_4{\cdot}H_2O$ [Me = Mn, Fe, Co, Ni, Zn]. *Neues Jahrbuch für Mineralogie Monatshefte*, **1991**, 296–306.

Witzke T., Wegner R., Doering T., Pöllmann H. and Schuckmann W. (2000) Serrabrancaite, $MnPO_4{\cdot}H_2O$, a new mineral from the Alto Serra Branca pegmatite, Pedra Lavrada, Paraiba, Brazil. *American Mineralogist*, **85**, 847–849.